The topology of the charge distribution and the electricfield gradient at the N nucleus in imines and diimides

Yossien Aray and Juan Murgich

Citation: The Journal of Chemical Physics **97**, 9154 (1992); doi: 10.1063/1.463341
View online: http://dx.doi.org/10.1063/1.463341
View Table of Contents: http://scitation.aip.org/content/aip/journal/jcp/97/12?ver=pdfcov
Published by the AIP Publishing

The topology of the charge distribution and the electric-field gradient at the N nucleus in imines and di-imides

Yossien Aray[a] and Juan Murgich[b]
Centro de Química, Instituto Venezolano de Investigaciones Científicas, Apartado 21827, Caracas 1020A, Venezuela

(Received 29 May 1991; accepted 1 September 1992)

A relationship between critical points that define the topology of the Laplacian of a molecular charge distribution $\nabla^2\rho(\mathbf{r})$, and components of the electric-field gradient (EFG) tensor at the nucleus of the two-coordinated N, obtained from an *ab initio* molecular-orbital calculation, was found in di-imides (R–N=N–H with R=H, F, and CN) and imines (RHC=N–H with R=H, F, CN, and CH_3). The q_{zz} component of the EFG was found to be determined by the position and magnitude of the nonbonded charge concentration present in the N valence shell, as defined by a maximum in $-\nabla^2\rho(\mathbf{r})$. The orientation of the z axis of the tensor was determined to be associated with three local maxima in $-\nabla^2\rho(\mathbf{r})$ present in the N valence shell while the asymmetry parameter of the tensor was found to be related to saddle points of the N valence shell located above and below the molecular plane.

INTRODUCTION

The electric-field gradient (EFG) at the nuclei EFG is very sensitive to the molecular charge distribution so it has been extensively used in solids, liquids, and gases to study the chemical bonding, electronic substituent effects, degree of charge transfer, etc.[1] Generally, the interpretation of the EFG has been made in terms of the populations of localized orbitals centered at the atom containing the quadrupolar nucleus[1] or of molecular orbitals.[2] Nevertheless, the orbitals and their populations are not physical observables as defined by quantum mechanics.[3] The populations are not invariant under unitary transformations between sets of orbitals[3] so the information about the charge distribution obtained by means of these interpretations of the EFG are open to serious questions. Clearly, new and more rigorous ways of interpreting the EFG are required in order to obtain reliable data about the molecular charge distribution $\rho(\mathbf{r})$. A more adequate way of obtaining information is the interpretation of the EFG directly in terms of $\rho(\mathbf{r})$. One of the main reasons behind this approach is that $\rho(\mathbf{r})$ is a well-defined physical observable and it is independent of the orbital model used in its calculation.[3] Moreover, the information about $\rho(\mathbf{r})$ obtained from such an interpretation can be compared directly with that gathered by, i.e., x-ray diffraction at very low temperatures.[4] Such a check of $\rho(\mathbf{r})$ obtained with different techniques will be of great help in obtaining realistic molecular charge distributions. Additionally, the determination of the relationship between $\rho(\mathbf{r})$ and the EFG components will provide a new way of obtaining data on the charge distribution even for large molecules where adequate molecular-orbital (MO) calculations are not feasible with present day computers.

It is known that from the $\rho(\mathbf{r})$ distribution, one cannot determine directly the regions where the electronic shells are located.[3] In the analysis of the EFG, this point is a significant shortcoming because most of the gradient arises from the shells of the atom containing the quadrupolar nucleus.[1,5] It is clear, then, that a method capable of locating the atomic shells is required for an interpretation of the EFG in terms of $\rho(\mathbf{r})$. One of the methods used in the location of the atomic charge density involves the use of the Laplacian $\nabla^2\rho(\mathbf{r})$ distribution.[3] Such a method takes advantage of the sensitivity of the second derivatives to the spatial variations of $\rho(\mathbf{r})$ in order to locate the regions of space occupied by the electronic shells. Bader and co-workers[3] found that the $\nabla^2\rho(\mathbf{r})$ distribution shows that the valence shell in a light free atom is a sphere on whose surface $\rho(\mathbf{r})$ is maximal and, we have to add, in atoms without nucleus with a quadrupole moment, it is also uniform. The formation of covalent bonds produces a number of small local maxima and minima in each valence shell with characteristics and symmetry that are a function of the number and nature of the intervening atoms.[3] As the EFG present at the nucleus reflects the asymmetry in the charge distribution of the atomic shells, a connection between the extremes in the $\nabla^2\rho(\mathbf{r})$ of the valence shell and the gradient at the quadrupole nucleus is likely to exist at least for light atoms. Recently, such a relationship was found for the monocoordinated N atoms in nitriles.[5] In the present work, we have studied this association in the two-coordinated N atoms found in di-imides [RN(2)=N(1)H with R=H, F, and CN] and imines [RHC=N(1)H with R=H, F, CN, and CH_3].

Bader and co-workers[3] have also shown that the surfaces of zero flux in $\nabla\rho(\mathbf{r})$ define regions of space containing nuclei that can be assigned to chemical atoms. Such a definition of atoms in molecules, based only on the properties of $\rho(\mathbf{r})$, allows a detailed and unambiguous analysis of the contributions of different parts of the molecular system to the EFG found at quadrupolar nuclei.[5] In the present work, we have applied such an analysis to imines and di-imides in order to evaluate each of the contributions to the total EFG found at the N nuclei.

[a]On leave from the Departamento de Química, Facultad Experimental de Ciencias, Universidad del Zulia, Maracaibo, Venezuela.
[b]To whom the correspondence should be addressed.

 0021-9606/92/249154-07$06.00

TABLE I. EFG components at the N atom in CH_2=NH in the molecular principal inertia axis. MW corresponds to the values measured by microwave spectroscopy while TZP to a triple-ζ basis set. Also indicated are the number of configurations employed in the CI method. All quantities are in atomic units.

Method	Basis set	$-E$ (a.u.)	q_{zz}	q_{yy}	q_{xx}	q_{xz}	Ref.
MW	...	...	−0.228	0.893	−0.665	...	12
SCF	TZP (58 GTO)	94.0642	−0.225	0.918	−0.663	0.623	12
MCSCF[a]	TZP	n.a.	−0.218	0.849	−0.631	n.a.	12
CI	TZP	94.3759	−0.220	0.846	−0.626		12
SCF	6–13G** (45 GTO)	94.0357	−0.184	0.811	−0.627	0.586	this work
CI[b]	TZP	94.1985	−0.246	0.852	−0.606	0.582	this work

[a]35 585 configuration.
[b]59 321 configuration.

COMPUTATIONAL METHODS

The *ab initio* self-consistent-field (SCF) MO calculations were performed on an IBM 3090 computer and an IBM RISC 6000 model 530 workstation using the HONDO-8 program[6] with a 6–31 G** and a triple-ζ (TZP) basis set.[7] Configuration-interaction (CI) calculations using single to triple excitations were carried out with the TZP set using the SIRIUS program[6] for a set of representative molecules. Experimental or optimized values for the bond lengths and bond angles were used when available.[8] For R=F and CN in di-imides as well as for R=CH_3 and F in imines, optimized geometries were obtained by the SCF gradient method with the 6–31G** basis set. The topological properties of the Laplacian of $\rho(\mathbf{r})$ were calculated with a locally modified version of the AIMPAC package.[9]

TABLE II. Principal components of the EFG tensor q_{ii}, asymmetry parameter η, and the angle θ between the principal z axes and the line joining the maximum found in the N "lone pair" and the N nucleus for a set of molecules described in the text. All quantities are in atomic units.

Method	Basis set	q_{zz}	q_{yy}	q_{xx}	η	θ	Ref.
		H_2C=NH					
SCF	6–31G**	−1.032	0.811	0.221	0.57	34.6	
SCF	TZP	−1.115	0.918	0.197	0.65	35.9	
CI[a]	TZP	−1.035	0.852	0.183	0.65	36.4	
CI	TZP	−1.031	0.816	0.215	0.58		12
		FHC=NH					
	6–31G**	−0.855	0.534	0.321	0.25	40.4	
SCF	TZP	−0.954	0.667	0.287	0.40	41.4	
CI[b]	TZP	−0.840	0.560	0.279	0.33	43.1	
		HN=NH					
SCF	6–31G**	−1.252	1.070	0.182	0.71	36.1	
SCF	TZP	−1.356	1.189	0.167	0.75	36.2	
CI[c]	TZP	−1.254	1.077	0.176	0.72	36.7	

[a]59 321 configuration.
[b]344 616 configuration.
[c]31 270 configuration.

BASIS-SETS TRUNCATION AND ELECTRON CORRELATION EFFECTS

The EFG is a traceless, symmetric second-rank tensor[1] whose principal axes are chosen such that its components q_{ii} satisfy $|q_{zz}| \geq |q_{yy}| \geq |q_{xx}|$. Usually, the quadrupole coupling constant, e^2qQ/h (Q equals the nuclear electric quadrupole moment, and $eq=q_{zz}$) plus the asymmetry parameter, $\eta=|(q_{yy}-q_{xx})/q_{zz}|$ are determined experimentally. There are several sources of uncertainty in both the measured as well as in the calculated EFG values that have to be analyzed when comparisons are made.[1] On one side, the lack of a reliable value of Q for ^{14}N prevented for a long time the unambiguous determination of q_{zz} from the measured coupling constants (Q values obtained with different experimental techniques were found to differ[10] by as much as 10% while those deduced from MO calculations[11] by up to 15%). Depending on the value of Q employed, the fitting with the experiment can be significantly improved[11] (or *worsened*). Then, in order to make meaningful comparisons, it is necessary to state the value of Q used in obtaining the EFG and to estimate the other possible sources of discrepancy between calculated and measured values.

The EFG values measured in the gaseous phase by microwave (MW) spectroscopy are averaged by the intramolecular vibrations[1] while the calculated ones are obtained, in general, for a rigid molecule. It has been estimated that the averaging produced by the intramolecular vibrations, in a molecule such as formaldoxime,[12] only changes the EFG components by about 2%. Consequently, the vibrational averaging of the EFG components appears to be of minor importance in molecules such as the imines and di-imides and can be neglected.

The deficiencies produced by the use of finite basis sets and the neglecting of the electron correlation in the MO calculations introduce uncertainties[11] in the EFGs. In order to assess them, MO calculations were performed in a set of three different molecules (CH_2=NH, FHC=NH, and HN=NH) with the 6–31G**, and the triple-ζ sets with and without using the CI method. In Table I are shown the calculated and measured EFG values obtained for CH_2=NH, the only molecule of this set for which experimental data exist.[13] In this table, the value of Q employed by Palmer and co-workers[13] was used to obtain the

TABLE III. Basis-set and CI effects on the nonbonded maxima of the N valence shell. The values shown correspond to the $\nabla^2\rho(\mathbf{r})$ at the local nonbonded maximum found in the N valence shell. All quantities are in atomic units.

Molecule	6–31G**	TZP	TZP+CI
H_2C=NH	3.443	3.157	2.993
FHC=NH	3.183	2.919	2.734
HN=NH	3.935	3.633	3.437

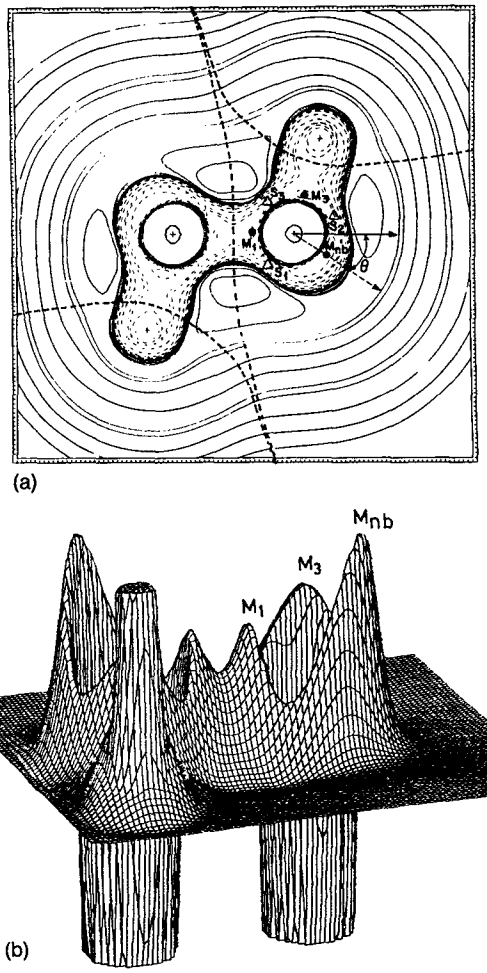

FIG. 1. Contour map of the Laplacian of the charge density for HN=NH in a plane that contains all the nuclei. Positive values are denoted by the solid contours, negative values by dashed contours. The contour values in a.u. are ± 0.002, ± 0.004, ± 0.008, increasing in powers of ten to 8.000. The outermost contour is $+0.002$ a.u. The intersection of the interatomic surface of zero flux in $\nabla\rho(\mathbf{r})$ with the plane of the figure (thick dashed lines), the position of the maxima in the $\nabla^2\rho(\mathbf{r})$ distribution of N(1) valence shell M_1, M_{nb}, and M_3 and of the saddle points S_i with $i=1$, 2, and 3 plus the angle θ are also shown. (b) Relief contour of the $-\nabla^2\rho(\mathbf{r})$ distribution in the same plane of Fig. (a) from HN=NH. The contribution of the N atomic cores has been omitted for clarity. The contribution of the H atom bonded to the N(1) has also been deleted to improve the display of the local maximum M_3 of the N(1) valence shell. The two bonding maxima M_1 and M_3 are observed in the region of the N(1)=X and N(1)–H bonds, respectively, plus a nonbonded maximum in the N(1) valence shell M_{nb}.

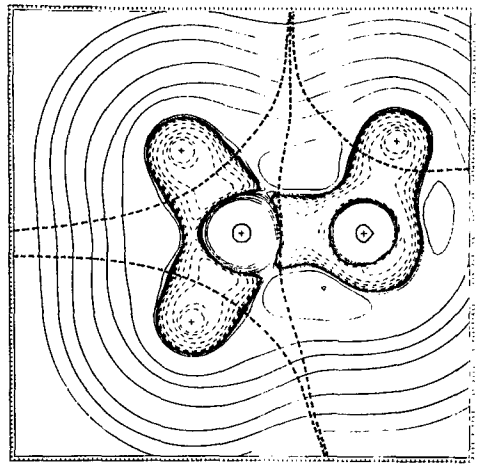

FIG. 2. Contour map of the $-\nabla^2\rho(\mathbf{r})$ distribution for the H2C=NH in a plane that contains all the nuclei. The parameters and other characteristics are equal to those of Fig. 1(a).

EFG from the MW data. The measured[13] and calculated EFG components in the principal inertia axes using double- and triple-ζ sets differ by about 3%–10% except for the q_{zz} component calculated with the 6–31G** set where a difference of 16% was found. It is interesting to note, nevertheless, that the trend observed upon substitution in the EFG values calculated with the triple ζ were faithfully reproduced by both the 6–31G** set and the TZP CI calculation as seen in Table II. The use of the TZP basis set and of the TZP plus the CI method for CH_2=NH produced a better fit for q_{zz} than the 6–31G** set but generated a worse one for the q_{yy} and q_{xx} components. In general, the differences found in Table I are equal or lower than those determined in other calculations in multiple-bonded N-containing compounds[11–14] except perhaps for q_{zz} calculated with the 6–31G** set in the inertia axis (probably a basis-set effect).

No experimental data were found for the other two remaining molecules so in Table II are shown the components calculated in the principal axes of the N EFG tensors for the complete set. Except for q_{xx}, the agreement between the 6–31G** and TZP CI values was quit remarkable ($<5\%$). It is important to notice that the trends observed upon substitution in the EFG components determined with both the TZP CI calculations and the 6–31G** basis set were remarkably similar.

The changes in the size of the basis set and the inclusion of the electron correlation modifies the molecular charge distribution.[3,15] Nevertheless, the number and the type of the critical points that define the topology of $\rho(\mathbf{r})$ in imines and di-imides was not altered by the inclusion of correlation or by extension of the basis set. As shown in Table III, the quantitative change in the Laplacian of $\rho(\mathbf{r})$ in one typical critical point such as the N "lone pair" by an increase in the basis set is quite constant ($\approx 8\%$). The electron correlation produced a similar variation in that maximum but it was smaller in ($\approx 5\%$–6%) magnitude. The tendency to have lower values in the $\nabla^2\rho(\mathbf{r})$ at the local maxima has been already observed for other compounds if larger basis sets or if the CI method was used.[15] It is interesting, nevertheless, to note that the trend observed in the values of the $\nabla^2\rho(\mathbf{r})$ at the critical points obtained with the TZP CI calculation is again well reproduced by the 6–31G** basis set.

Recently, it was found[11] that the truncation error resulting from the use of the 6–31G** set was very close but of different sign than the correlation correction in HCN and N_2. This led to a fortuitous cancellation of errors for this base that produced EFG values similar to those obtained with highly refined CI methods.[11] The similarity found in the trends in both the EFG and the Laplacian of

TABLE IV. Maxima of the $\nabla^2\rho(\mathbf{r})$ of the valence shell of the N atoms. The value of r is the distance from the local extremes to the N nucleus and θ is the angle between the C–N direction and the line joining the nucleus and the extreme in the valence shell [see Fig. 1(a)]. N(1) and N(2) represent the N atoms shown in Figs. 1(a) and 2. All quantities are in atomic units.

		M_1			M_{nb}			M_3		
R	Atom	r	θ	$\nabla^2\rho(\mathbf{r})$	r	θ	$\nabla^2\rho(\mathbf{r})$	r	θ	$\nabla^2\rho(\mathbf{r})$
					di-imides					
H	N(1)	0.816	127.0	2.133	0.722	51.8	3.895	0.796	126.6	2.328
F	N(1)	0.825	128.2	1.989	0.723	51.8	3.709	0.795	127.9	2.322
	N(2)	0.789	145.6	2.694	0.714	38.8	4.342	0.876	111.5	0.749
CN	N(1)	0.821	126.8	2.002	0.718	53.3	4.056	0.788	129.0	2.528
	N(2)	0.808	130.8	2.176	0.720	49.3	3.963	0.829	119.6	1.592
					imines					
H	N(1)	0.803	134.1	2.219	0.728	50.6	3.440	0.810	121.4	1.954
F	N(1)	0.815	129.8	2.015	0.731	50.3	3.224	0.812	121.8	1.897
CN	N(1)	0.806	129.0	2.151	0.725	51.0	3.590	0.805	121.3	2.069
CH_3	N(1)	0.804	132.2	2.271	0.730	52.4	3.351	0.810	121.8	2.088

$\rho(\mathbf{r})$ in the test set plus the results obtained by Cremer and Krüger[11] shows that the use of the 6–31G** set provides a reasonable compromise between the required accuracy in the EFG components, the values of $\rho(\mathbf{r})$ and the available computer time. For these reasons, this set was employed in the calculations of the other molecules studied in this work.

THEORY

The topological properties of $\rho(\mathbf{r})$ are displayed by its $\nabla\rho(\mathbf{r})$ and $\nabla^2\rho(\mathbf{r})$ fields.[3] Every gradient path originates and terminates at a critical point (CP) in $\rho(\mathbf{r})$, where $\nabla\rho(\mathbf{r})=0$. The CPs are classified by the eigenvalues[3] λ_i ($i=1$, 2, and 3) of the Hessian matrix $[H_{ij}=\partial^2\rho(\mathbf{r})/\partial\mathbf{x}_i\partial\mathbf{x}_j]$. In the di-imines and imides, only two of critical points exist that labeled by their rank (number of nonzero eigenvalues) and signature[3] (excess number of positive over negative eigenvalues) are $(3,-1)$ and $(3,-3)$. A $(3,-3)$ point is a local maximum, while a $(3,-1)$ (saddle point) represents local maxima in two directions and a local minimum in the third one. The $(3,-3)$ points occur generally at the nuclear positions[3] so that each nucleus is a point attractor in the $\nabla\rho(\mathbf{r})$ field. The region transversed by the gradient paths which terminate at a given nucleus constitutes its basin. The trajectories associated with λ_1 and λ_2 at each $(3,-1)$ point located between basins define the zero-flux surfaces S_{ij} that partition the molecule into unique fragments that are assigned to chemical atoms.[3]

As mentioned above, the $\nabla^2\rho(\mathbf{r})$ distribution readily identifies the atomic regions wherein the charge is locally concentrated $[\nabla^2\rho(\mathbf{r})<0]$ or depleted $[\nabla^2\rho(\mathbf{r})>0]$ thus providing a much enhanced view of the local form[3] of $\rho(\mathbf{r})$. The spherical valence shell described by the $\nabla^2\rho(\mathbf{r})$ distribution in an isolated atom is perturbed upon chemical combination and small local extremes in $\rho(\mathbf{r})$ are created on it.[3,16] These extremes were found to be one of the main sources of the EFG found at the one-coordinated N nucleus in nitriles.[5]

RESULTS AND DISCUSSION

In Figs. 1 and 2 are shown the distribution of $\nabla^2\rho(\mathbf{r})$ in HN=NH and in H_2C=NH in the nuclear plane. In both cases, the N(1) atom has a "double bond" with a N [N(2)] or C atom plus a "single" bond with a H atom. In each two-coordinated N atom, there are three local maxima in the $\nabla^2\rho(\mathbf{r})$ distribution of its valence shell, all of them located in the nuclear plane. One of the maxima corresponds to a bonded concentration along the "double" bond N=X (M_1) while another belongs to the "single" N–H (or R) (M_3) bond. The remaining maximum (M_{nb}) corresponds to the classical N "lone pair." The position and values of $\nabla^2\rho(\mathbf{r})$ at the maxima in the N(1) and N(2) valence shells are shown in Table IV. In addition to the maxima found in the N valence shell, three saddle points are found in the nuclear plane plus two additional ones located symmetrically below and above this plane.

The relationship of the zz component of the N EFG with $\rho(\mathbf{r})$ may be explored by relating it with the extremes of the $\nabla^2\rho(\mathbf{r})$ distribution of the N valence shells.[5,14] The EFG in an isolated molecule may be divided into the electronic contribution of the atom containing the quadrupolar nucleus plus a nuclear and an electronic contribution from the remaining atoms.[5] In this work, we have used the atoms uniquely defined by the zero-flux surfaces[3] to calculate the different contributions to the EFG at the N nuclei. Examples of the zero-flux surfaces used in this work are shown in Fig. 1. In Table V–VII are shown the components of the total EFG tensor and each of the different contributions calculated in imines and di-imides. In these tables, we see that the total q_{zz} ($q_{zz}|_{\text{tot}}$) is determined mainly by the electrons of the basin of the N atom where the EFG is calculated. If one plots the value of $q_{zz}|_{\text{tot}}$ vs the values of $\nabla^2\rho(\mathbf{r})$ at the local maxima (M_{nb}, M_1, or M_3), a linear correlation is found at M_{nb} with $r=0.988$ (also at M_3 with $r=0.914$) but none at M_1. A multiple linear regression calculated with the values of $\nabla^2\rho(\mathbf{r})$ found at maxima M_{nb}, M_1, and M_3 and $q_{zz}|_{\text{tot}}$ ($r=0.991$) showed

TABLE V. Calculated values of q_{zz} at the N nuclei. The notation is such that for the di-imides, we have that RN(2)=N(1)H and for the imines that RHC=N(1)H. Then $q_{zz}|_{tot}$ is the total value of the q_{zz} component at the N nucleus while $q_{zz}|_N$ is that produced by the N basin where the field gradient has been calculated, $q_{zz}|_R$ is the total contribution from all the atoms forming the molecule except the N where the EFG is calculated, $q_{zz}|_\alpha$ with α=N(1), N(2), H, and C is the contribution from these neighboring atoms while $q_{zz}|_S$ is that of the neighboring H, F, and CN fragments at the N(2) nucleus. All quantities are in atomic units.

di-imides

R	N atom	$q_{zz}\|_{tot}$	$q_{zz}\|_N$	$q_{zz}\|_R$	$q_{zz}\|_{N(2)}$	$q_{zz}\|_H$
H	N(1)	−1.207	−1.215	0.008	0.003	0.016
F	N(1)	−1.115	−1.137	0.022	−0.014	0.005
CN	N(1)	−1.328	−1.346	0.018	−0.007	−0.013
R	N atom	$q_{zz}\|_{tot}$	$q_{zz}\|_N$	$q_{zz}\|_R$	$q_{zz}\|_{N(1)}$	$q_{zz}\|_S$
H	N(2)	−1.207	−1.215	0.008	0.003	0.016
F	N(2)	−1.431	−1.549	0.118	0.118	−0.011
CN	N(2)	−1.181	−1.180	−0.001	0.039	−0.029

imines

R	N atom	$q_{zz}\|_{tot}$	$q_{zz}\|_N$	$q_{zz}\|_R$	$q_{zz}\|_C$	$q_{zz}\|_H$
H	N(1)	−0.997	−1.028	0.031	0.056	−0.021
F	N(1)	−0.855	−0.885	0.030	0.032	−0.016
CN	N(1)	−1.113	−1.128	0.015	0.029	−0.016
CH_3	N(1)	−0.961	−0.972	0.011	0.037	−0.025

that the only important contribution arises from the M_{nb} maximum. The other two terms produce a negligible contribution indicating that only the "lone pair" is responsible for this component of the EFG.

The contribution of the rest of the molecule ($q_{zz}|_R$) to the N $q_{zz}|_{tot}$ in imines and di-imides is only a few percent or less of its value except for the F–N(2)=NH case where

TABLE VI. Calculated values of q_{yy} at the N nuclei. The notation is identical to that used in Table V. All quantities are in atomic units.

di-imides

R	N atom	$q_{yy}\|_{tot}$	$q_{yy}\|_N$	$q_{yy}\|_R$	$q_{yy}\|_{N(2)}$	$q_{yy}\|_H$
H	N(1)	1.026	1.189	−0.163	−0.077	−0.011
F	N(1)	0.881	1.047	−0.166	−0.090	0.005
CN	N(1)	1.157	1.322	−0.165	−0.071	−0.014
R	N atom	$q_{yy}\|_{tot}$	$q_{yy}\|_N$	$q_{yy}\|_R$	$q_{yy}\|_{N(1)}$	$q_{yy}\|_S$
H	N(2)	1.026	1.189	−0.163	−0.077	−0.011
F	N(2)	0.906	0.989	−0.083	−0.036	−0.004
CN	N(2)	0.703	0.871	−0.168	−0.078	−0.076

imines

R	N atom	$q_{yy}\|_{tot}$	$q_{yy}\|_N$	$q_{yy}\|_R$	$q_{yy}\|_C$	$q_{yy}\|_H$
H	N(1)	0.765	1.018	−0.253	−0.173	−0.077
F	N(1)	0.534	0.796	−0.262	−0.189	−0.081
CN	N(1)	0.896	1.154	−0.258	−0.171	−0.081
CH_3	N(1)	0.699	0.981	−0.282	−0.184	−0.091

TABLE VII. Calculated values of q_{xx} at the N nuclei. The notation is identical to that used in Table V. All quantities are in atomic units.

di-imides

R	N atom	$q_{xx}\|_{tot}$	$q_{xx}\|_N$	$q_{xx}\|_R$	$q_{xx}\|_{N(2)}$	$q_{xx}\|_H$
H	N(1)	0.181	0.026	0.154	0.073	0.022
F	N(1)	0.234	0.091	0.143	0.103	−0.110
CN	N(1)	0.171	0.023	0.148	0.079	0.027
R	N atom	$q_{xx}\|_{tot}$	$q_{xx}\|_N$	$q_{xx}\|_R$	$q_{xx}\|_{N(1)}$	$q_{xx}\|_S$
H	N(2)	0.181	0.026	0.154	0.073	0.022
F	N(2)	0.465	0.560	−0.094	−0.082	0.001
CN	N(2)	0.478	0.310	0.168	0.039	0.105

imines

R	N atom	$q_{xx}\|_{tot}$	$q_{xx}\|_N$	$q_{xx}\|_R$	$q_{xx}\|_C$	$q_{xx}\|_H$
H	N(1)	0.232	0.013	0.219	0.117	0.098
F	N(1)	0.321	0.088	0.233	0.158	0.097
CN	N(1)	0.216	−0.026	0.242	0.143	0.097
CH_3	N(1)	0.261	−0.009	0.270	0.146	0.115

it is near 8%. In principle, one may expect an important contribution to $q_{zz}|_{tot}$ from the two neighboring atoms bonded to the N. Nevertheless, as seen in Table V, their contributions are quite small and, in most cases, have different signs so they tend to cancel each other.

The large difference between the contributions from the rest of the molecule and from the basin of the N atom $q_{zz}|_N$ arises from several factors. The $q_{zz}|_R$ component contains contributions from both the electronic and the nuclear charges. In general, these contributions are more or less of the same order of magnitude but have a different sign so they nearly cancel each other. On the other hand, the electronic contribution from $q_{zz}|_N$ is not compensated by any nuclear charge so its full contribution is present in the EFG. The r^{-3} factor present in the EFG operator[1] further enhances the contribution of the electrons located in the basin of the atom containing the quadrupolar nucleus. It is for these two reasons that even relatively small variations in $\rho(\mathbf{r})$ of the N basin produce noticeable changes in $q_{zz}|_{tot}$.

The analysis of the asymmetry parameter is much more complicated because the three diagonal components of the EFG are included in the definition of η. In principle, we may expect, as in the q_{zz} component, that the N valence density will prevail so it determines the value of η. Alternatively, the rest of the molecule may overcome the valence-shell contribution and determine the value of η. From Tables VI and VII we see that the contributions to $q_{yy}|_{tot}$ and $q_{xx}|_{tot}$ from the atoms bonded to the N are far from being negligible as in the q_{zz} case. The most important difference between q_{xx} and q_{yy} is found in the relative weight of the contributions of the N basin and the rest of the molecule in each of them. In the N(1) atoms, the N basin contribution is larger than $q_{yy}|_R$ by a factor between 3 and 8 while $q_{xx}|_N$ is only just a fraction (3%–64%) of $q_{xx}|_R$. For the N(2) atoms, the values of $q_{yy}|_N$ are 5–12

times larger in magnitude than those of $q_{yy}|_R$. The value of $q_{xx}|_N$ for N(2) is smaller than the contribution from the rest of the molecule for R=H but the opposite is true for R=F and CN. If we recall its definition, for the N(1) we have then that $\eta \cong |q_{xx}|_R - q_{yy}|_N - q_{yy}|_R|/|q_{zz}|_N|$. Recalling that the $q_{zz}|_N$ component has only a small nonlocal contribution, we may conclude that η in this atom is determined by the combined action of both local and nonlocal contributions to q_{xx} and q_{yy} but weighted by q_{zz}. For N(2), a similar result may be obtained so we may conclude that, in imines and di-imides, η will be quite sensitive to changes in the rest of the molecule if the weighting factor q_{zz} does not change markedly.

Aside from the study of the atomic contribution to the total EFG, it is interesting to search for phenomenological relationships between some of the critical points of the $\nabla^2\rho(\mathbf{r})$ that describe the charge topology with components of the EFG. The largest spatial variation in the charge density of the N valence shell in the imines and di-imides is in the direction or very near the maximum of the uncompensated "lone pair" as seen in Fig. 1. We found that the z axis in N(1) does not point directly toward the lone pair maximum M_{nb} but it is slightly shifted by the other maxima present in the N valence shell (see Table IV). If one plots the angle θ related to the EFG z axis direction and shown in Fig. 1 vs the ratio $(M_1-M_3)/M_{nb}$ of the $\nabla^2\rho(\mathbf{r})$ values found at these local maxima, a linear correlation with $r=0.996$ is found for the N(1) in both the di-imides and the imines. This correlation indicates that the direction of the z axis at the N(1) is affected by the difference in the charge concentrations of the valence shell along the N–H and N=X bonds weighted by the concentration found at the lone pair. If one substitutes X, the entire N(1) valence shell is modified because the nonlocal nature of the shell polarizability.[3] Upon substitution, a different set of $\nabla^2\rho(\mathbf{r})$ values at M_1, M_{nb}, and M_3 appears in the N shell. Depending on the type of changes introduced by the substituent, the new orientation of the z axis will reflect the substituent ability to modify the N atomic charge distribution.

The asymmetry parameter is an indicator of the distortion of the charged distribution around the quadrupolar nucleus. From Figs. 1 and 2, it is seen that the charge of the N(1) valence shell tends to be concentrated in the nuclear plane as shown by the position of the maxima M_{nb}, M_1, and M_3. Such a trend in this part of the N shell produces a relative decrease in the concentration above and below the nuclear plane that generates two saddle points in the $\nabla^2\rho(\mathbf{r})$ distribution. In monocoordinated N atoms, the values of η were found to be linearly correlated with a rather complex function of the $\nabla^2\rho(\mathbf{r})$ values found at the saddle points (SP) located in a plane perpendicular to the C–N axis.[5] A search of a similar relationship for the N(1) showed that, in imines and di-imides, η exhibited a linear correlation ($\eta=-1.171$ SP$+1.100$, $r=0.977$) with the $\nabla^2\rho(\mathbf{r})$ values found in these two saddle points located above (or below) the nuclear plane. This correlation shows that a lower value of $\nabla^2\rho(\mathbf{r})$ at the saddle point indicates a larger deviation of the shell distribution from the spherical symmetry and consequently produces a larger η.

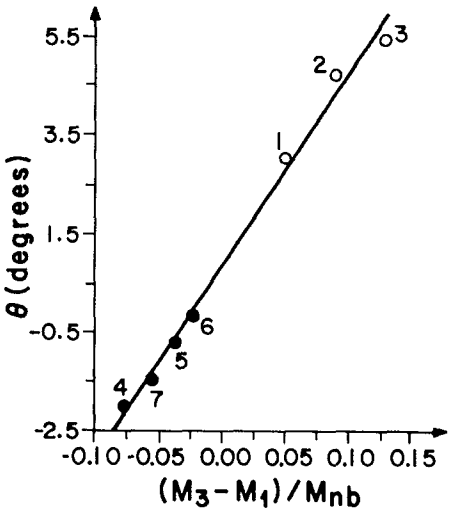

FIG. 3. Plot of the angle θ [shown in Fig. 1(a)] vs the ratio of the $\nabla^2\rho(\mathbf{r})$ values $(M_1-M_3)/M_{nb}$ for the N(1) in imines and di-imides. The open circles correspond to RN=N(1)H while the full ones to RHC=N(1)H. We have also in the figure that H=1, F=2, CN=3, H=4, F=5, CN=6, and CH3=7 while the straight line correspnds to $\theta=0.891+38.436(M_1-M_3)/M_{nb}$ with $r=0.996$.

CONCLUSIONS

In the two-coordinated N atoms, the nonbonded charge concentration found in its valence shell (lone pair) determines the value of q_{zz}, while the asymmetry parameter contains also some contributions from the charges of the rest of the molecule. A correlation between the values of the $\nabla^2\rho(\mathbf{r})$ found at local maxima of the valence shell with the orientation of the z axes and between the asymmetry parameter and the values of the $\nabla^2\rho(\mathbf{r})$ at the saddle points of the valence shell was found for the N atom. The above results show that the use of the $\nabla^2\rho(\mathbf{r})$ distribution in molecules allows the interpretation of the EFG components directly in terms of topology of an observable such as $\rho(\mathbf{r})$ without the use of quantities without a precise physical meaning such as the Mulliken orbital populations.

ACKNOWLEDGMENT

We want to thank the Centro Científico of IBM de Venezuela C.A. for a generous grant of computer time.

[1] E. A. C. Lucken, *Nuclear Quadrupole Coupling Constants* (Academic, New York, 1969); J. A. S. Smith, Chem. Soc. Rev. **15**, 225 (1986).
[2] F. A. Cotton and C. B. Harris, Proc. Natl. Acad. Sci. U.S.A. **56**, 12 (1966).
[3] R. F. W. Bader, T. T. Nguyen-Dang, and Y. Tal, Rep. Prog. Phys. **44**, 895 (1984); R. F. W. Bader, *Atoms in Molecules: A Quantum Theory* (Oxford University, Oxford, 1990).
[4] R. Destro, R. Bianchi, and G. Morosi, J. Phys. Chem. **93**, 4447 (1989).
[5] Y. Aray, and J. Murgich, J. Chem. Phys. **91**, 293 (1989).
[6] HONDO 8 and SIRIUS are from the MOTECC™ package, IBM Center for Scientific and Engineering Computations, Kingston, NY 12401.
[7] R. Ditchfield, W. J. Hehre, and J. A. Pople, Chem. Phys. **54**, 724 (1970).
[8] The geometry of HN=NH is from A. Lathan, L. A. Curtis, W. J. Hehre, J. B. Lisle, and J. A. Pople, Prog. Phys. Org. Chem. **11**, 175 (1974) while that of H_2C=NH is from R. Macualey, L. A. Burnelle, and C. Sandorfy, Theor. Chim. Acta **29**, 11 (1973) and for

NCHC=NH is from J. B. Moffat, J. Chem. Soc. Chem. Commun. **21**, 888 (1975).
[9] F. W. Biegler-König, R. F. W. Bader, and T. T. Nguyen-Dang, J. Comput. Chem. **3**, 317 (1982).
[10] N. Ensllin, W. Bertozzi, S. Kowalski, C.P. Sargent, W. Turchinetz, C. F. Williamson, S. P. Pivozinsky, J. W. Lightbody, and S. Penner, Phys. Rev. C **9**, 1705 (1974); H. Winter and Andrä, Phys. Rev. A **21**, 581 (1980).
[11] D. Cremer and M. Krüger, J. Phys. Chem. **96**, 3239 (1992).
[12] A. Klesig and D. H. Sutter, Z. Naturforsch. **44a**, 1063 (1989).
[13] H. Krause, D. H. Sutter, and M. H. Palmer, Z. Naturforsch. **45a**, 817 (1990).
[14] Y. Aray, H. Soscun, and J. Murgich, Int. J. Quant. Chem. **25**, 587 (1991).
[15] C. Gatti, P. J. MacDougall, and R. F. W. Bader, J. Chem. Phys. **88**, 3792 (1988); R. J. Boyd and L. C. Wang, J. Comput. Chem. **10**, 367 (1989).